JCTC Journal of Chemical Theory and Computation

Article

pubs.acs.org/JCTC

Comparative Assessment of DFT Performances in Ru- and Rh-Promoted σ-Bond Activations

Yuanyuan Sun, Lianrui Hu, and Hui Chen*

Beijing National Laboratory for Molecular Sciences (BNLMS), CAS Key Laboratory of Photochemistry, Institute of Chemistry, Chinese Academy of Sciences, Beijing 100190, China

Supporting Information

ABSTRACT: In this work, the performances of 19 density functional theory (DFT) methods are calibrated comparatively on Ru- and Rh-promoted σ-bond (C−H, O−H, and H−H) activations. DFT calibration reference is generated from explicitly correlated coupled cluster CCSD(T)-F12 calculations, and the 4s4p core−valence correlation effect of the two 4d platinum group transition metals is also included. Generally, the errors of DFT methods for calculating energetics of Ru-/Rh-mediated reactions appear to correlate more with the magnitude of energetics itself than other factors such as metal identity. For activation energy calculations, the best performing functionals for both Ru and Rh systems are MN12SX < CAM-B3LYP < M06-L < MN12L < M06 < ωB97X < B3LYP < LC-ωPBE (in the order of increasing mean unsigned deviations, MUDs, of less than 2 kcal/mol). For reaction energy calculations, best functionals with MUDs less than 2 kcal/mol are PBE0 < CAM-B3LYP ≈ N12SX. The effect of the DFT empirical dispersion correction on the performance of the DFT methods is beneficial for most density functionals tested in this work, reducing their MUDs to different extents. After including empirical dispersion correction, ωB97XD, B3LYP-D3, and CAM-B3LYP-D3 (PBE0-D3, B3LYP-D3, and ωB97XD) are the three best performing DFs for activation energy (reaction energy) calculations, from which B3LYP-D3 and ωB97XD can notably be recommended uniformly for both the reaction energy and reaction barrier calculations. The good performance of B3LYP-D3 in quantitative description of the energetic trends further adds value to B3LYP-D3 and singles this functional out as a reasonable choice in the Ru/Rh-promoted σ-bond activation processes.

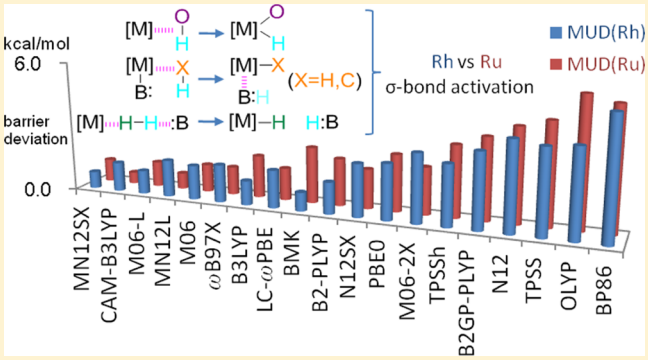

1. INTRODUCTION

Because of their characteristics of high reactivity, high selectivity, and good functional-group tolerance often displayed in catalysis, the platinum group metals (PGMs: ruthenium, osmium, rhodium, iridium, palladium, and platinum) play very important roles in organometallic chemistry and catalysis.[1−38] Currently, exploiting various chemical reactivities promoted by many PGMs constitutes a substantial portion of the research in these areas. The reactions catalyzed by PGMs cover an extremely wide range including C-C/C-heteroatom coupling, carbonylations, oxidations, hydrosilylations, hydrogenations, etc. For many of these reactions to proceed, H−H, C−H, and O−H activations are crucial steps.

Among PGMs, Ru and Rh have gotten special attentions for their multifarious catalytic activities.[15−38] Despite them not being present within the same group in the periodic table, Ru and Rh in some structurally similar catalytic systems can interestingly promote similar chemical transformation involving H−H, C−H, and O−H σ-bond activations, which gave the initial inspiration to conduct the current comparative study. As shown in reactions 1 of Scheme 1, both Ru and Rh can promote the activation of the aromatic C−H bond to produce the metallacyclic intermediate, which is the key step in chelation-assisted oxidative cyclization of the ortho aromatic substrates with alkenes or alkynes.[30,39,40] The difference between Ru and Rh catalysts is the neutral arene (*p*-cymene in experiments) ligand for Ru and the anionic cyclopentadienyl (Cp or Cp* in experiments) ligand for Rh, which also match their oxidation states of Ru(II) and Rh(III), respectively. This ligand difference also exists in important Ru(II) and Rh(III) hydrogenation systems,[41−58] as shown in reactions 2 and 3 of Scheme 1. Two different H_2 activation modes exist in these hydrogenation systems, namely, ligand-assisted H−H cleavage (reactions 2) and external base-assisted H−H cleavage (reactions 3). Both are important steps in corresponding hydrogenation catalysis to generate the key metal hydride species used in substrate hydrogenation, which have been widely studied in theoretical modeling.[44,55,59−61] For O−H cleavage, oxidative addition type reactions promoted by Ru(0) and Rh(I) metal centers can also take place with quite similar phosphine rich ligating environments, as shown in reactions 4

Received: October 14, 2014
Published: February 20, 2015

DOI: 10.1021/ct5009119
J. Chem. Theory Comput. 2015, 11, 1428−1438

Scheme 1. Ru/Rh-Promoted σ-Bond Activation Reactions Studied in This Work

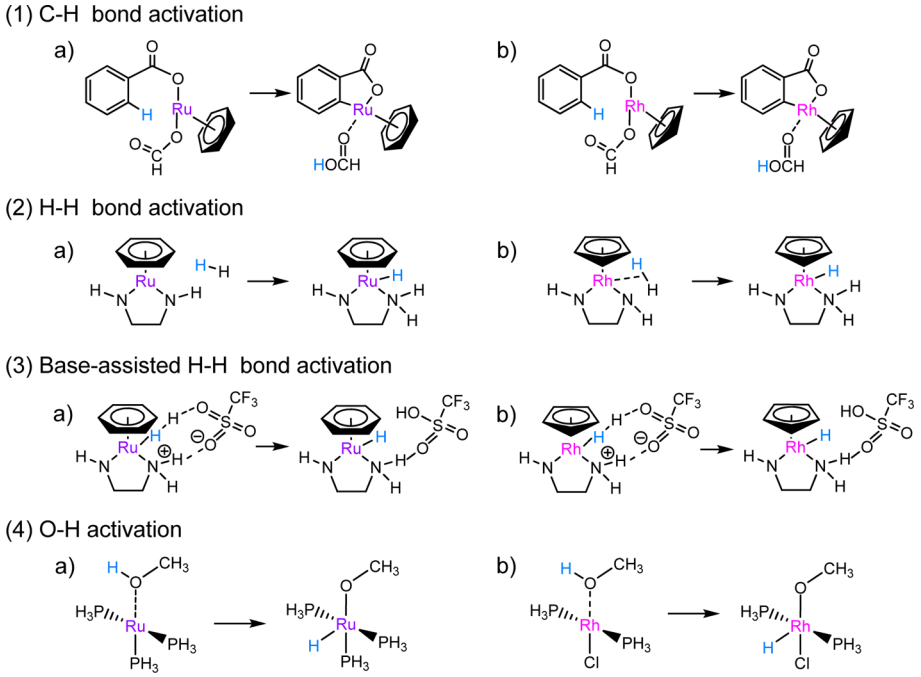

of Scheme 1. This process is considered to be crucial in the aerobic N-alkylation reactions of amides and amines with alcohols.[62,63]

Density functional theory (DFT) has achieved significant success in the field of transition metal chemistry.[64−74] Due to the wide occurrence of Ru- and Rh-catalyzed reactions, more accurate DFT treatment and modeling are highly desirable. With the development of various new density functionals (DFs), calibration studies for these DFs are absolutely necessary for many users of DFT methods from both computational and experimental communities to select more appropriate DFs for Ru and Rh systems. Correspondingly, there have been a few studies devoted to the calibration of DFs on several important Ru- or Rh-catalyzed reactions. In 2007, Grimme et al. used the QCISD(T) method as reference to compare the performances of several DFs on an olefin metathesis reaction catalyzed by a Grubbs first-generation Ru catalyst.[75] For this well-known olefin metathesis reaction, recently Truhlar and his co-workers employed the CCSD(T) method as reference to assess the DFT performances with a Grubbs second-generation Ru catalyst.[76] In 2010, Neese and his co-workers calibrated two commonly used DFs (BP86 and B3LYP) in the whole catalytic cycle of a relatively large Rh(I)-catalyzed olefin hydrogenation reaction system bearing a well-studied bidentate phosphorus ligand, using a local coupled cluster method (LPNO−CCSD) as reference.[77] Concerning the very representative Ru-catalyzed water oxidation reaction that has been extensively explored, very recently we conducted a DFT calibration study on the corresponding whole catalytic cycle with the CCSD(T) method as reference.[78] All of these previous DFT calibration studies focused on some important but specific reactions promoted by Ru or Rh, while a comparative study between similar reactions with similar catalysts of these two metals is still missing so far.

Concerning limited comparative studies of different metals with similar coordinate environments, recently we reported our DFT calibration results on C−H activations promoted by the late PGMs (Rh, Pd, Ir, and Pt) in a series of pincer complexes,[79] in which we observed some uniform trends for the accuracy of almost all tested DFT methods. An interesting phenomenon is that the DFT barriers for C−H activation reactions involving Rh pincer complexes are more accurate than those involving Pd pincer complexes. Understanding this result is intriguing, which also prompts us to explore whether the systematic trend of DFT performance exists in a variety of σ-bonds activations promoted by Ru and Rh within PGMs.

In this work, the activation energies and reaction energies of σ-bond activations by Ru and Rh catalysts as depicted in Scheme 1 were investigated, which includes O−H, C−H, and H−H σ-bond activations. High level reference values were calculated through the explicitly correlated CCSD(T)-F12 method, which was developed for alleviating the slow basis set convergence often encountered in traditional coupled cluster calculation, and the Ru/Rh 4s4p outer-core electron-correlation effect was also considered. The DFs under calibration cover a wide range from pure GGA and meta-GGA to hybrid and double hybrids, including PBE0,[80] M06,[81] M06-L,[81a] M06-2X,[81] TPSS,[82] TPSSh,[82] B3LYP,[83] B2GP-PLYP,[84] B2-PLYP,[85] ωB97X,[86] OLYP,[87] BMK,[88] BP86,[89] CAM-B3LYP,[90] LC-ωPBE,[91] N12,[92] MN12-L,[93] N12-SX,[94] and MN12-SX.[94] Differing from our previous work,[78,79,95−99] here we also tested several new Minnesota functionals developed and made available very recently, such as N12, MN12-L, N12-SX, and MN12-SX.

2. COMPUTATIONAL DETAILS

All DFT calculations were performed with the Gaussian 09 software package.[100] The commonly used DFT functional B3LYP was employed to optimize the geometric structures of all the minima and transition states in conjunction with cc-pVTZ/cc-pV(T+d)Z[101,102] and cc-pVTZ-PP[103] basis sets on the main group atoms H,C,N,O,F/P,S,Cl and transition metals (Ru, Rh), respectively. Meanwhile, the scalar relativistic effect was taken into account using the Stuttgart new relativistic

DOI: 10.1021/ct5009119
J. Chem. Theory Comput. 2015, 11, 1428−1438

Table 1. Activation Energies $\Delta E^{\ddagger}$ and Reaction Energies ΔE (in kcal/mol) at Various CCSD(T)-F12b Levels for Ru/Rh-promoted O−H Bond Activation (Reactions 4 in Scheme 1)

reactions	$\Delta E^{\ddagger}_{ADZ}$	$\Delta E^{\ddagger}_{ATZ}$	$\Delta E^{\ddagger}_{CBS(ADZ-ATZ)}$	ΔE_{ADZ}	ΔE_{ATZ}	$\Delta E_{CBS(ADZ-ATZ)}$
4a (Ru_{OH})	13.73	13.54	13.37	−18.32	−17.93	−17.75
4b (Rh_{OH})	21.99	21.91	21.83	9.42	9.96	10.29

energy-consistent small-core pseudopotential (PP) ECP28MDF in combination with the above basis set for Ru and Rh.[103] Harmonic vibrational frequencies were calculated to ensure that all of the minima and transition states have no and one proper imaginary frequency, respectively.

Hereafter, DZ/TZ/QZ are used as the abbreviations of double/triple/quadruple-ζ quality basis sets (such as cc-pVDZ/cc-pVTZ/cc-pVQZ), while augmented double/triple/quadruple-ζ quality basis sets with diffuse functions (such as aug-cc-pVDZ/aug-cc-pVTZ/aug-cc-pVQZ) are abbreviated as ADZ/ATZ/AQZ. In these abbreviations, for second row atoms (P, S, and Cl), the "n+d" revision of the corresponding standard correlation consistent basis set cc-pVnZ basis set, labeled as cc-pV(n+d)Z basis set,[102] which was generated from the corresponding standard correlation consistent basis set by adding one additional high-exponent *d* function for getting better behaved convergence in basis set extrapolation, is used throughout this work. The activation energies and the reaction energies were calculated with respect to the reactant complexes. On the basis of the B3LYP/DZ optimized structures, the activation energies and the reaction energies calculated at single point B3LYP level with TZ and QZ basis sets were compared. Among all the reactions promoted by Ru and Rh in Scheme 1, the maximum differences between TZ and QZ basis sets for the activation energies and reaction energies are 0.34 and 0.56 kcal/mol (see Table S1 in Supporting Information document), respectively, which indicates that for DFT methods TZ basis sets are accurate enough for the energetics calculations of the reaction systems explored in this work. The effect of empirical dispersion correction was evaluated using Grimme's DFT-D3 method,[104] and the zero short-range damping scheme DFT-D3(0) was employed.[104,105] There are no DFT-D3(0) parameters for the ωB97X functional and the four new Minnesota functionals of N12, MN12-L, N12-SX, and MN12-SX. For ωB97X, the empirical dispersion corrected functional ωB97XD by its original developers was used instead.[106]

All single-point ab initio wave function theory (WFT) calculations using the explicitly correlated coupled cluster F12 method (CCSD(T)-F12) were carried out with the MOLPRO program package.[107] The CCSD(T)-F12 approach employing the valence-only correlated CCSD(T)-F12b method with the diagonal fixed amplitude 3C(FIX) *ansatz* was performed for all of the reaction systems.[108,109] There is no direct F12 correction to perturbative triples (T), and the triple energy contribution was not scaled by the factor of MP2-F12/MP2 in all CCSD(T)-F12b calculations. In the CCSD(T)-F12b computations, density fitting of the Fock and exchange matrices used the auxiliary basis sets (ABSs), def2-AQZVPP/JKFIT,[110] cc-pVTZ/JKFIT, and aug-cc-pVTZ/JKFIT[111] for transition metals, H, and the rest of the atoms, respectively, while density fitting of the other two-electron integrals employed ABSs of aug-cc-pVTZ-PP/MP2FIT,[112] cc-pVTZ/MP2FIT, and aug-cc-pVTZ/MP2FIT[113] for metals (Ru, Rh), H, and the rest of the atoms. The resolution of the identity (RI) approximation with the complementary auxiliary basis set (CABS) approach[114] also used the same JKFIT ABSs in density fitting of the Fock and exchange matrices. The value of the germinal Slater exponent in the valence-only and core−valence correlated CCSD(T)-F12b calculations was taken to be 1.4 a_0^{-1}, as done in many previous studies.[78,95,96,115]

The orbital basis set used with the CCSD(T)-F12b method was ADZ basis sets for all atoms except hydrogen. The nonaugmented DZ basis set was adopted for H atoms, which was found to be sufficient in CCSD(T)-F12 computation.[109] To test the convergence of the basis set in CCSD(T)-F12b/ADZ calculations, complete basis set (CBS) limit extrapolation of CCSD(T)-F12b based on the ADZ and ATZ basis set pair for the relatively smaller Ru/Rh-promoted reaction systems (reactions 4 in Scheme 1) was conducted. The same auxiliary basis sets used in CCSD(T)-F12b/ADZ were adopted for CCSD(T)-F12b/ATZ computations. According to Schwenke's two-point CBS limit extrapolation scheme,[116] the CCSD-F12b correlation energy and perturbative triples (T) contribution were extrapolated separately using the following equation:

$$E_{corr,n} = E_{corr,CBS} + \frac{A}{n^{pow}} \quad (1)$$

The optimal parameter *pow* in the above equation was chosen to be 2.48307 for CCSD-F12b correlation energy and 2.7903 for perturbative triples (T) contribution, which was determined by Hill et al. for ADZ-ATZ extrapolation.[117] The HF CBS limit was approximated by the SCF+CABS-singles energy[118] computed by the largest basis set (ATZ) in CCSD(T)-F12b calculations.

The 4s4p outer-core valence electron correlation corrections for transition metals Ru and Rh were also taken into account through the CCSD(T)-F12b method to alleviate the potential basis set incompleteness error issue. The cc-pwCVDZ-PP basis set was used for metals,[103] and DZ basis sets were adopted for the rest of the atoms (this combination of basis sets is labeled as wDZ). The core−valence correlation correction was determined by the difference of two single point calculations with and without Ru/Rh 4s4p electrons correlated using the same wDZ basis set. The auxiliary basis sets used for Ru/Rh 4s4p core−valence correlation correction were selected according to the corresponding orbital basis sets, which have two differences from the auxiliary basis sets in the above valence-only electron correlation calculations. These differences lie in the fact that in core−valence electron correlation calculations (a) all diffuse auxiliary bases were not included; and that (b) cc-pwCVTZ-PP/MP2FIT instead of aug-cc-pVTZ-PP/MP2FIT was used for Ru and Rh.[119]

Considering both the valence-only electron correlation and the Ru/Rh 4s4p outer core−valence electron correlation, the final reference values of activation energies and reaction energies can be written as

$$\Delta E^{\ddagger}_{final} = \Delta E^{\ddagger}_{ADZ} + \Delta\Delta E^{\ddagger}_{4s4p} \quad (2)$$

$$\Delta E_{final} = \Delta E_{ADZ} + \Delta\Delta E_{4s4p} \quad (3)$$

where $\Delta E^{\ddagger}_{ADZ}/\Delta E_{ADZ}$ is obtained from the valence-only correlated CCSD(T)-F12b calculation, and $\Delta\Delta E^{\ddagger}_{4s4p}/$

DOI: 10.1021/ct5009119
J. Chem. Theory Comput. 2015, 11, 1428−1438

$\Delta\Delta E_{4s4p}$ is obtained from the metal 4s4p outer-core electron correlation correction for the activation energy/reaction energy.

3. RESULTS AND DISCUSSION

3.1. Reference Coupled Cluster Calculations. To test the accuracy of the reference values generated from CCSD(T)-F12b/ADZ calculations, CCSD(T)-F12b/CBS calculations with ADZ-ATZ CBS limit extrapolation for OH bond activation by Ru/Rh catalysts were performed, and the results are shown in Table 1. It can be seen that the activation energies obtained by ADZ are only 0.16 and 0.36 kcal/mol away from CBS values for Rh and Ru systems, respectively, while the corresponding deviations of the reaction energy (0.87 and 0.57 kcal/mol) are understandably larger than those of the activation energy (due to the larger electronic structure change from reactant to product than that from reactant to transition state) but still smaller than 1 kcal/mol. Therefore, based on the good basis set convergence, the activation energies and the reaction energies at the CCSD(T)-F12b/ADZ level can be relied on to calibrate the performance of different DFs. The results calculated at the CCSD(T)-F12b/ADZ level are summarized in Table 2. Hereafter, O−H, C−H, H−H, and external base-assisted H−H bond activation promoted by Ru/Rh will be labeled as Ru_{OH}/Rh_{OH}, Ru_{CH}/Rh_{CH}, Ru_{HH}/Rh_{HH}, and Ru_{HHeb}/Rh_{HHeb}. From these data, one can see that (1) comparing the corresponding reactions mediated by Ru and Rh, for C−H bond activation (reactions 1) and the external base-assisted H−H bond activation (reactions 3), the activation/reaction energies are close, but for O−H and direct H−H bond activations without external base (reactions 2 and 4), the activation/reaction energy differences between Ru- and Rh-mediated reactions are relatively large. (2) Comparing the two different mechanisms of H−H bond activation for one metal, direct H−H bond activation by Rh (reaction 2b) is comparable to the external base-assisted one by Rh (reaction 3b) concerning activation energy but not reaction energy, while for the Ru-promoted reaction the latter mechanism (reaction 3a) is much more favorable in activation energy than the former (reaction 2a). (3) The Ru/Rh 4s4p electron-correlation corrections for all the activation energies and reaction energies are smaller than 0.50 kcal/mol; thus, the core-correlation effect is quite limited for these 4d Ru/Rh systems studied in this work.

Table 2. Activation Energies $\Delta E^{\ddagger}$ and Reaction Energies ΔE Calculated at the CCSD(T)-F12b/ADZ Level and Their Ru/Rh 4s4p Correlation Corrections for All of the Reactions in Scheme 1 (in kcal/mol)

reactions	$\Delta E^{\ddagger}_{ADZ}$	$\Delta\Delta E^{\ddagger}_{4s4p}$	$\Delta E^{\ddagger}_{final}$	ΔE_{ADZ}	$\Delta\Delta E_{4s4p}$	ΔE_{final}
1a (Ru_{CH})	12.32	−0.21	12.11	−2.60	−0.16	−2.75
1b (Rh_{CH})	11.89	−0.15	11.73	−5.85	0.07	−5.78
2a (Ru_{HH})	20.22	0.02	20.24	−16.21	0.18	−16.03
2b (Rh_{HH})	4.98	−0.04	4.93	−35.52	0.30	−35.22
3a (Ru_{HHeb})	6.69	−0.13	6.56	5.10	−0.18	4.92
3b (Rh_{HHeb})	3.99	−0.01	3.99	0.15	0.09	0.24
4a (Ru_{OH})	13.73	−0.20	13.54	−18.32	−0.05	−18.37
4b (Rh_{OH})	21.99	−0.43	21.56	9.42	−0.49	8.94

3.2. DFT Calibration Results. *3.2.1. Activation Energies.* Using the above obtained activation energies $\Delta E^{\ddagger}_{final}$ as reference, the performances of 19 selected functionals were calibrated, and the results are shown in Table 3 and Figure 1a.

Table 3. Deviations of DFT-Computed Activation Energies (without Empirical Dispersion Correction) $\Delta E^{\ddagger}$ (kcal/mol) from the Reference Coupled Cluster Values $\Delta E^{\ddagger}_{final}$ [a]

	B3LYP	PBE0	BMK	BP86	CAM-B3LYP	M06-L	M06	M06-2X	TPSS	TPSSh	ωB97X	B2GP-PLYP	B2-PLYP	OLYP	LC-ωPBE	N12	N12SX	MN12L	MN12SX
1a(Ru_{CH})	−0.98	−3.87	2.95	−7.75	0.02	2.42	0.74	4.46	−4.47	−3.14	2.83	−3.94	−1.97	−5.42	−0.92	−6.52	−3.13	−0.22	1.35
1b(Rh_{CH})	−1.71	−4.44	−0.25	−7.63	−0.99	2.10	0.66	3.27	−4.50	−3.43	1.64	−3.13	−1.45	−5.04	−1.80	−6.53	−4.07	−2.76	−0.22
2a(Ru_{HH})	3.08	−1.42	2.79	1.33	0.14	0.78	−0.48	−0.11	3.09	2.01	−0.50	2.58	2.71	7.92	−2.20	2.13	0.13	1.40	1.37
2b(Rh_{HH})	−0.35	−2.15	−1.37	−1.68	−0.96	0.29	−0.04	−0.86	−0.35	−0.56	−0.97	0.30	0.09	−1.38	−2.37	−2.27	−2.75	−0.77	−0.59
3a(Ru_{HHeb})	−2.47	−3.36	2.47	−6.10	−0.98	−0.09	−0.07	1.04	−3.52	−2.69	0.83	−4.36	−2.98	−6.03	−0.67	−4.67	−2.44	−0.34	0.76
3b(Rh_{HHeb})	−2.26	−3.04	0.12	−4.39	−1.58	0.16	0.05	−1.42	−2.42	−2.05	−0.22	−2.39	−1.48	−4.03	−1.46	−3.21	−2.33	−1.36	−0.54
4a(Ru_{OH})	−1.20	−1.74	−2.04	−6.98	−0.93	−1.30	3.78	3.02	−7.47	−5.26	0.97	−4.05	−0.97	−3.97	−2.08	−3.86	−1.54	−0.94	0.71
4b(Rh_{OH})	−0.12	−0.56	1.66	−8.16	1.81	−1.75	5.49	6.96	−8.21	−5.08	4.06	−7.93	−2.77	−5.57	1.29	−4.27	−0.48	−1.82	1.74
MSD(Rh)[b]	−1.11	−2.54	0.04	−5.47	−0.43	0.20	1.54	1.99	−3.87	−2.78	1.13	−3.29	−1.40	−4.01	−1.08	−4.07	−2.41	−1.68	0.10
MUD(Rh)[b]	1.11	2.54	0.85	5.47	1.33	1.07	1.56	3.13	3.87	2.78	1.72	3.44	1.45	4.01	1.73	4.07	2.41	1.68	**0.77**
MSD(Ru)[c]	−0.39	−2.60	1.54	−4.88	−0.44	0.45	0.99	2.10	−3.09	−2.27	1.03	−2.44	−0.80	−1.87	−1.47	−3.23	−1.74	−0.03	1.04
MUD(Ru)[c]	1.93	2.60	2.56	5.54	**0.52**	1.15	1.27	2.16	4.64	3.27	1.28	3.73	2.16	5.84	1.47	4.29	1.81	0.73	1.04
MSD(tot)[d]	−0.75	−2.57	0.79	−5.17	−0.43	0.33	1.27	2.04	−3.48	−2.52	1.08	−2.87	−1.10	−2.94	−1.28	−3.65	−2.07	−0.85	0.57
MUD(tot)[d]	1.52	2.57	1.71	5.50	0.93	1.11	1.41	2.64	4.25	3.03	1.50	3.59	1.80	4.92	1.60	4.18	2.11	1.20	**0.91**

[a]The smallest MUD values are shown in bold font. [b]MUD and MSD values for Rh-promoted reactions. [c]MUD and MSD values for Ru-promoted reactions. [d]MUD and MSD values for all the reactions in Scheme 1 mediated by Rh and Ru.

DOI: 10.1021/ct5009119
J. Chem. Theory Comput. 2015, 11, 1428−1438

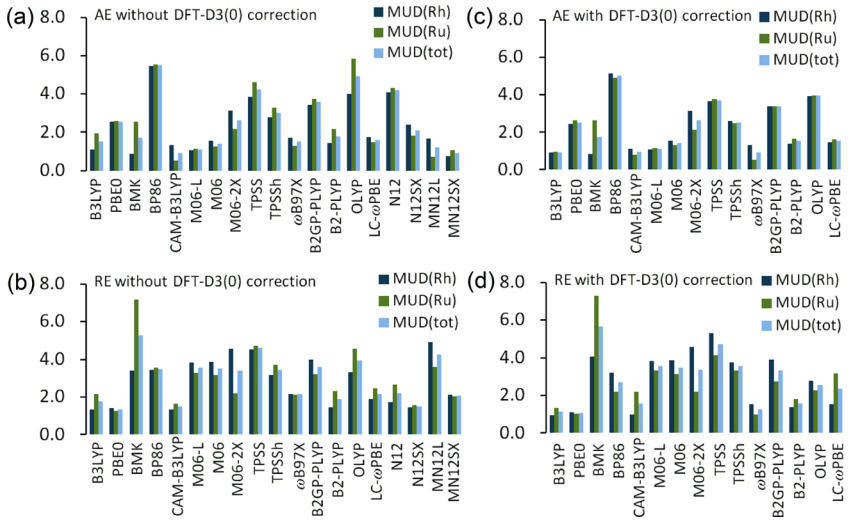

Figure 1. Mean unsigned deviations (MUD) of the calculated activation energies (AE) and reaction energies (RE) for all reactions in Scheme 1 with and without DFT dispersion corrections (in kcal/mol).

Mean unsigned deviations (MUDs) in kcal/mol were analyzed over three sets of data, i.e., MUD(Ru) averaged over Ru-mediated reactions, MUD(Rh) averaged over Rh-mediated reactions, and MUD(tot) averaged over all the reactions under study. From Table 3 and Figure 1a one can see that, the differences between MUD(Rh) and corresponding MUD(Ru) for almost all tested DFs are less than 1 kcal/mol with just a few exceptions (BMK and OLYP), which indicates the similar performances of the DFs in Ru- and Rh-promoted σ-bond activation reactions. The smallest deviations are produced by MN12SX (0.77) for Rh-mediated reactions, CAM-B3LYP (0.52) for Ru-mediated reactions, and MN12SX (0.91) for all the reactions. DFs with all the three MUDs less than 2 kcal/mol are MN12SX < CAM-B3LYP < M06-L < MN12L < M06 < ωB97X < B3LYP < LC-ωPBE (in the order of increasing MUD(tot)). The largest MUDs are produced by BP86 (5.47) for Rh-mediated reactions, OLYP (5.84) for Ru-mediated reactions, and BP86 (5.50) for all the reactions. In view of the two largest MUDs(tot) produced by BP86 and OLYP, they are not suitable DFs to compute the activation energies of Rh/Ru-mediated reactions. B3LYP was found to perform best (MUD = 1.17) in our previous work on C−H activation by various pincer complexes of late PGMs (Rh, Pd, Ir, and Pt).[79] Here for Rh-mediated reactions in this work, despite not being the best one, B3LYP also performs well with MUD(Rh) of 1.11 kcal/mol. The MUDs(tot) of B3LYP, PBE0, TPSS, TPSSh, ωB97X, and B2-PLYP are close to their corresponding MUDs for the C−H activation by the late PGM (Rh, Pd, Ir, and Pt) pincer complexes in our previous work (with differences less than 1 kcal/mol),[79] indicating the stable performance of these functionals for most PGMs.

In our previous study on C−H activation by various pincer complexes of late PGMs (Rh, Pd, Ir, and Pt),[79] we observed that for all tested DFs, the accuracy of activation energy calculations for Rh is higher than that for Pd. It is intriguing to know the origin of this trend, and if the whole set of 4d PGMs (Ru, Rh, Pd) have a uniform trend in DFT calculation accuracy. First, from the DFT results of Ru and Rh systems in this work, their accuracies of activation energy calculations are comparable, and thus there is no apparent trend for Ru and Rh. Concerning the origin of the trend observed in our previous study, we note that the magnitudes of C−H activation energies of various Pd pincer complexes were consistently much larger than the corresponding ones of Rh pincer complexes.[79] Thus, the performance trend in Rh and Pd pincer systems is in accord with the order of the magnitudes of activation energies. Generally, for a functional, the lower activation energy tends to have smaller error than the higher activation energy. This is due to the fact that the magnitude of activation energy is also a measurement of electronic structure difference between transition state and reactant. Higher activation energy corresponds to larger difference in electronic structure, which is more difficult to describe accurately with DFs and could hence lead to larger error. This viewpoint is also consistent with the Ru and Rh systems under study because there is no consistent magnitude trend of the activation energies between them. Therefore, the magnitude of reaction energy appears to significantly affect the DFT performance.

3.2.2. Reaction Energies. The performances of different DFs in calculating reaction energies were also investigated, and the results are illustrated in Table 4 and Figure 1b. Compared with MUDs(tot) for the corresponding activation energies, MUDs(tot) of most tested functionals for reaction energy increase to various extents, and the decreased MUDs(tot) values are produced only by PBE0, BP86, OLYP, N12, and N12SX. Functionals with MUDs(tot) increased by more than 1 kcal/mol are BMK, M06-L, M06, and MN12L; while functionals with MUDs(tot) decreased by more than 1 kcal/mol are PBE0, BP86, and N12. The difference between the MUD(Rh) and MUD(Ru) for the same functional also becomes much larger for reaction energy than for activation energy. Considering both MUD(Rh) and MUD(Ru), there are only three functionals with both MUDs smaller than 2 kcal/mol, which are PBE0, CAM-B3LYP, and N12SX. BMK is found to be the worst performing DF for reaction energy, with a MUD(tot) of 5.28 kcal/mol, which might be attributed to the fact that this functional was designed and optimized for activation energy calculation rather than reaction energy calculation.

3.2.3. Effects of DFT Empirical Dispersion Correction. The DFT calibration results of the activation energies after adding the DFT empirical dispersion corrections are collected in Table 5 and depicted in Figure 1c. After taking account of the DFT empirical dispersion correction, MUDs(Rh) decreased to different degrees (maximum improvement of 0.42 kcal/mol

DOI: 10.1021/ct5009119
J. Chem. Theory Comput. 2015, 11, 1428−1438

Table 4. Deviations of DFT-Computed Reaction Energies (without Empirical Dispersion Correction) ΔE (kcal/mol) from the Reference Coupled Cluster Values ΔE_{final}[a]

	B3LYP	PBE0	BMK	BP86	CAM-B3LYP	M06-L	M06	M06-2X	TPSS	TPSSh	ωB97X	B2GP-PLYP	B2-PLYP	OLYP	LC-ωPBE	N12	N12SX	MN12L	MN12SX
1a (Ru_{CH})	1.52	−0.84	5.56	−0.77	1.21	6.79	2.47	2.30	2.63	2.27	2.78	−1.04	−0.19	−0.26	0.03	−0.49	−0.25	0.81	0.65
1b (Rh_{CH})	1.16	−1.05	2.10	0.50	−0.07	7.48	2.63	−0.43	3.77	2.83	1.10	1.05	1.31	1.14	−1.45	0.57	−0.93	−1.43	−1.00
2a (Ru_{HH})	3.37	0.04	4.09	5.74	−0.53	4.55	1.93	−1.97	7.99	5.56	−1.51	5.37	2.92	11.22	−2.10	5.90	2.19	2.29	2.43
2b (Rh_{HH})	−0.51	−0.97	−2.91	3.83	−2.98	5.21	2.20	−5.19	5.47	3.34	−3.33	5.79	1.74	3.11	−3.77	2.35	−1.26	−0.79	−0.68
3a (Ru_{HHeb})	−2.23	−2.89	4.59	−5.05	−0.44	0.72	−0.25	1.18	−1.87	−1.36	1.19	−6.26	−3.64	−6.61	−0.20	−3.30	−1.18	−0.83	0.87
3b (Rh_{HHeb})	−2.71	−3.08	1.50	−2.75	−2.12	2.10	−0.71	−3.47	0.12	−0.32	−1.02	−3.18	−1.41	−4.62	−2.07	−1.30	−1.51	−3.04	−1.72
4a (Ru_{OH})	−1.50	−1.21	−14.36	−2.70	−4.47	1.13	8.01	3.31	−6.37	−5.61	−3.05	−0.12	2.57	0.20	−7.53	1.00	−2.59	−10.44	−4.24
4b (Rh_{OH})	−1.03	−0.60	−7.13	−6.61	0.21	−0.50	9.90	9.18	−8.71	−6.22	3.16	−5.88	−1.43	−4.39	−0.22	−2.62	−2.05	−14.47	−5.04
MSD(Rh)[b]	−0.77	−1.42	−1.61	−1.26	−1.24	3.57	3.50	0.02	0.16	−0.09	−0.02	−0.55	0.05	−1.19	−1.88	−0.25	−1.44	−4.93	−2.11
MUD(Rh)[b]	1.35	1.42	3.41	3.42	**1.34**	3.82	3.86	4.57	4.52	3.18	2.15	3.98	1.47	3.31	1.88	1.71	1.44	4.93	2.11
MSD(Ru)[c]	0.29	−1.23	−0.03	−0.70	−1.06	3.30	3.04	1.20	0.59	0.21	−0.15	−0.51	0.41	1.14	−2.45	0.78	−0.46	−2.04	−0.07
MUD(Ru)[c]	2.15	**1.25**	7.15	3.57	1.66	3.30	3.17	2.19	4.72	3.70	2.13	3.20	2.33	4.57	2.47	2.67	1.55	3.59	2.05
MSD(tot)[d]	−0.24	−1.33	−0.82	−0.98	−1.15	3.44	3.27	0.61	0.38	0.06	−0.09	−0.53	0.23	−0.03	−2.16	0.26	−0.95	−3.49	−1.09
MUD(tot)[d]	1.75	**1.34**	5.28	3.49	1.50	3.56	3.51	3.38	4.62	3.44	2.14	3.59	1.90	3.94	2.17	2.19	1.50	4.26	2.08

[a]The smallest MUD values are shown in bold font. [b]MUD and MSD values for Rh-promoted reactions. [c]MUD and MSD values for Ru-promoted reactions. [d]MUD and MSD values for all of the reactions in Scheme 1 mediated by Rh and Ru.

from ωB97XD) for almost all tested functionals except for the BMK and M06 series of functionals with unchanged MUDs(Rh). For Ru-mediated reactions, only two functionals (CAM-B3LYP and LC-ωPBE) increased MUDs(Ru) by more than 0.1 kcal/mol but still smaller than 0.3 kcal/mol (maximum increase of 0.27 kcal/mol from CAM-B3LYP). All of the other functionals were either almost unaffected by varying MUD(Ru) within 0.1 kcal/mol (PBE0, BMK, and M06 series) or substantially improved by about 1−2 kcal/mol (maximum MUD(Ru) lowering of 1.86 kcal/mol from OLYP). Combining MUD(Rh) and MUD(Ru), upon addition of DFT empirical dispersion correction, the MUDs(tot) of BMK, CAM-B3LYP, PBE0, and M06 series remained almost unchanged by having a variation within 0.05 kcal/mol, while MUDs(tot) of the rest of the functionals were substantially decreased. Functionals with all three MUDs less than 2 kcal/mol are ωB97X < B3LYP < CAM-B3LYP < M06-L < M06 < B2-PLYP < LC-ωPBE (in the order of increasing MUD(tot)). Except for B2-PLYP, the other six functionals are among the eight best performing DFs without DFT empirical dispersion correction. The best performing DF ωB97XD here with the DFT empirical dispersion correction (MUD(tot) of 0.91 kcal/mol) has a very close MUD to the best one without empirical dispersion correction (MN12SX with MUD(tot) of 0.91 kcal/mol). With DFT-D3(0) correction, BP86 still performs worst by having the largest MUD(tot) of 5.03 kcal/mol, which implies again that this functional should be avoided in reactions barrier calculations. MUD variation of a functional between Ru- and Rh-mediated reactions with DFT empirical dispersion correction becomes smaller in comparison with the corresponding variation without DFT empirical dispersion correction.

The effect of DFT empirical dispersion correction for reaction energies is illustrated in Table 6 and depicted in Figure 1d. The DFs with MUDs(Rh) decreased by more than 0.3 kcal/mol are B3LYP, PBE0, CAM-B3LYP, ωB97X, OLYP, and LC-ωPBE, while DFs with MUDs(Rh) increased by more than 0.3 kcal/mol are BMK, TPSS, and TPSSh. DFs with MUDs(Ru) decreased by more than 0.3 kcal/mol are B3LYP, BP86, TPSS, TPSSh, ωB97X, B2GP-PLYP, B2-PLYP, and OLYP, while DFs with MUDs(Ru) increased by more than 0.3 kcal/mol are CAM-B3LYP and LC-ωPBE. Thus, for some DFs like CAM-B3LYP, LC-ωPBE, TPSS, and TPSSh, DFT-D3(0) dispersion correction does not show uniform direction of effect on Rh/Ru-promoted reactions. Overall, DFs with all three MUDs less than 2 kcal/mol are PBE0 < B3LYP < ωB97X < B2-PLYP (in the order of increasing MUD(tot)). We note that as far as reaction energies are concerned, PBE0 is the best performing DFs both with and without DFT empirical dispersion correction. As is the case without empirical dispersion correction, BMK seems to be the worst performing DF by having an MUD(tot) of 5.67 kcal/mol.

3.2.4. Correlation Analysis for the Trend Performance of DFT. To explore the trends of DFT-computed energetics, a correlation analysis between the DFT results and the reference CCSD(T)-F12 data was performed. For reaction barrier and reaction energy, the correlation analysis results for eight best-performing functionals with the smallest MUDs(tot) (selected from the MUD data with DFT dispersion correction except the four new Minnesota functionals N12, N12SX, MN12L, and MN12SX) are shown in Figures 2 and 3, respectively. First we can see that the correlations R^2 are at least 0.94 in both activation energy and reaction energy trend analysis, which

DOI: 10.1021/ct5009119
J. Chem. Theory Comput. 2015, 11, 1428−1438

Table 5. Deviations of DFT-Computed Activation Energies (with DFT Empirical Dispersion Correction) $\Delta E^{\ddagger}$ (kcal/mol) from the Reference Coupled Cluster Values $\Delta E^{\ddagger}_{final}$[a]

	B3LYP	PBE0	BMK	BP86	CAM-B3LYP	M06-L	M06	M06-2X	TPSS	TPSSh	ωB97X	B2GP-PLYP	B2-PLYP	OLYP	LC-ωPBE
1a (Ru_{CH})	−0.16	−3.42	3.90	−6.76	0.58	2.42	0.77	4.46	−3.79	−2.49	0.77	−3.61	−1.51	−4.25	−0.33
1b (Rh_{CH})	−1.18	−4.13	0.34	−7.04	−0.64	2.10	0.70	3.27	−4.09	−3.02	−0.24	−2.93	−1.17	−4.47	−1.42
2a (Ru_{HH})	1.00	−2.63	0.55	−1.11	−1.24	0.82	−0.65	−0.07	1.37	0.34	−0.72	1.80	1.61	2.74	−3.67
2b (Rh_{HH})	−0.13	−2.02	−1.16	−1.34	−0.84	0.28	−0.03	−0.86	−0.09	−0.36	−0.96	0.37	0.19	−1.24	−2.25
3a (Ru_{HHeb})	−1.18	−2.60	3.75	−4.42	−0.23	−0.11	0.05	1.03	−2.26	−1.56	0.05	−3.92	−2.38	−4.07	0.15
3b (Rh_{HHeb})	−1.83	−2.82	0.62	−3.72	−1.35	0.15	0.01	−1.43	−1.94	−1.67	−0.92	−2.22	−1.28	−3.42	−1.21
4a (Ru_{OH})	−1.46	−1.88	−2.38	−7.31	−1.12	−1.31	3.79	3.02	−7.68	−5.46	0.56	−4.18	−1.13	−4.88	−2.27
4b (Rh_{OH})	−0.47	−0.77	1.28	−8.52	1.56	−1.73	5.46	6.98	−8.46	−5.35	3.08	−8.06	−2.97	−6.54	1.03
MSD(Rh)[b]	−0.91	−2.44	0.27	−5.16	−0.32	0.20	1.54	1.99	−3.65	−2.60	0.24	−3.21	−1.31	−3.92	−0.96
MUD(Rh)[b]	0.91	2.44	**0.85**	5.16	1.10	1.07	1.55	3.13	3.65	2.60	1.30	3.40	1.40	3.92	1.48
MSD(Ru)[c]	−0.45	−2.63	1.45	−4.90	−0.50	0.45	0.99	2.11	−3.09	−2.29	0.17	−2.48	−0.85	−2.61	−1.53
MUD(Ru)[c]	0.95	2.63	2.64	4.90	0.79	1.16	1.32	2.14	3.77	2.46	**0.53**	3.37	1.66	3.98	1.60
MSD(tot)[d]	−0.68	−2.53	0.86	−5.03	−0.41	0.33	1.26	2.05	−3.37	−2.45	0.20	−2.84	−1.08	−3.27	−1.25
MUD(tot)[d]	0.93	2.53	1.75	5.03	0.94	1.11	1.43	2.64	3.71	2.53	**0.91**	3.38	1.53	3.95	1.54

[a]The smallest MUD values are shown in bold font. [b]MUD and MSD values for Rh-promoted reactions. [c]MUD and MSD values for Ru-promoted reactions. [d]MUD and MSD values for all of the reactions in Scheme 1 mediated by Rh and Ru.

Table 6. Deviations of DFT-Computed Reaction Energies (with Empirical Dispersion Correction) ΔE (kcal/mol) from the Reference Coupled Cluster Values ΔE_{final}[a]

	B3LYP	PBE0	BMK	BP86	CAM-B3LYP	M06-L	M06	M06-2X	TPSS	TPSSh	ωB97X	B2GP-PLYP	B2-PLYP	OLYP	LC-ωPBE
1a (Ru_{CH})	2.10	−0.44	6.00	−0.10	1.61	6.83	2.65	2.33	3.16	2.78	1.50	−0.86	0.11	0.65	0.46
1b (Rh_{CH})	1.39	−0.85	2.14	0.72	0.08	7.52	2.79	−0.40	4.00	3.05	0.15	1.09	1.39	1.39	−1.28
2a (Ru_{HH})	1.66	−0.91	2.08	3.80	−1.70	4.57	1.87	−1.95	6.67	4.25	−0.87	4.67	1.95	5.99	−3.34
2b (Rh_{HH})	0.02	−0.63	−2.54	4.61	−2.70	5.19	2.32	−5.21	6.10	3.86	−2.13	5.92	1.93	3.04	−3.47
3a (Ru_{HHeb})	0.09	−1.53	6.98	−2.21	1.01	0.72	−0.02	1.18	0.20	0.58	0.63	−5.42	−2.48	−2.44	1.36
3b (Rh_{HHeb})	−0.67	−1.88	3.62	−0.24	−0.82	2.11	−0.51	−3.46	1.94	1.38	−1.10	−2.43	−0.38	−0.87	−0.68
4a (Ru_{OH})	−1.46	−1.24	−14.12	−2.72	−4.40	1.12	7.91	3.30	−6.46	−5.66	−0.98	−0.04	2.65	0.05	−7.46
4b (Rh_{OH})	−1.71	−1.00	−7.88	−7.32	−0.27	−0.50	9.83	9.20	−9.21	−6.74	2.80	−6.14	−1.81	−5.83	−0.73
MSD(Rh)[b]	−0.24	−1.09	−1.17	−0.56	−0.93	3.58	3.61	0.03	0.71	0.39	−0.07	−0.39	0.28	−0.57	−1.54
MUD(Rh)[b]	**0.95**	1.09	4.04	3.22	0.97	3.83	3.86	4.57	5.31	3.76	1.55	3.89	1.38	2.78	1.54
MSD(Ru)[c]	0.60	−1.03	0.23	−0.31	−0.87	3.31	3.10	1.22	0.89	0.49	0.07	−0.42	0.56	1.06	−2.24
MUD(Ru)[c]	1.32	1.03	7.29	2.21	2.18	3.31	3.11	2.19	4.12	3.32	**0.99**	2.75	1.80	2.28	3.16
MSD(tot)[d]	0.18	−1.06	−0.47	−0.43	−0.90	3.45	3.36	0.62	0.80	0.44	0.00	−0.40	0.42	0.25	−1.89
MUD(tot)[d]	1.14	**1.06**	5.67	2.71	1.57	3.57	3.49	3.38	4.72	3.54	1.27	3.32	1.59	2.53	2.35

[a]The smallest MUD values are shown in bold font. [b]MUD and MSD values for Rh-promoted reactions. [c]MUD and MSD values for Ru-promoted reactions. [d]MUD and MSD values for all of the reactions in Scheme 1 mediated by Rh and Ru.

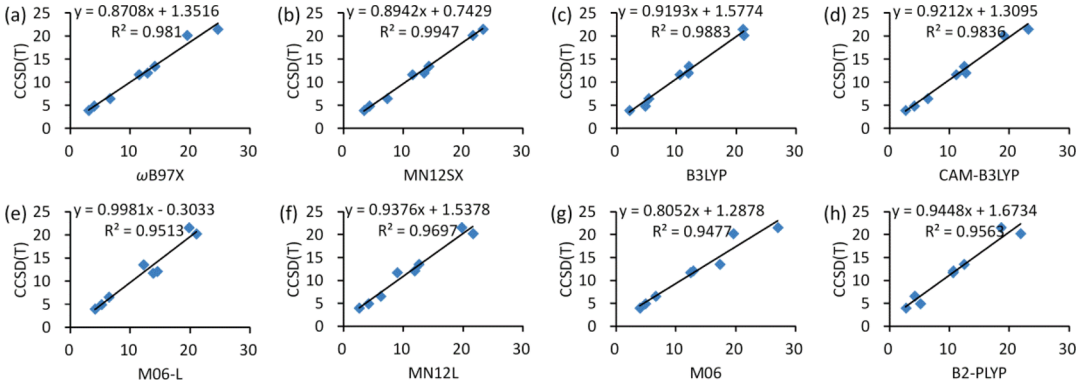

Figure 2. Correlation between reference coupled cluster and DFT (with the eight smallest MUDs after DFT dispersion correction) results for activation energy.

means that DFT can reliably follow the qualitative trends in reaction barrier and reaction energy computations. In activation energy trend analysis, the slope of the correlation line for M06-L is close to ideal 1.0 (deviation within 0.0019 from 1.0), and the intercept of the correlation line (0.3 kcal/mol) is also negligible. In reaction energy trend analysis, the functional

DOI: 10.1021/ct5009119
J. Chem. Theory Comput. 2015, 11, 1428−1438

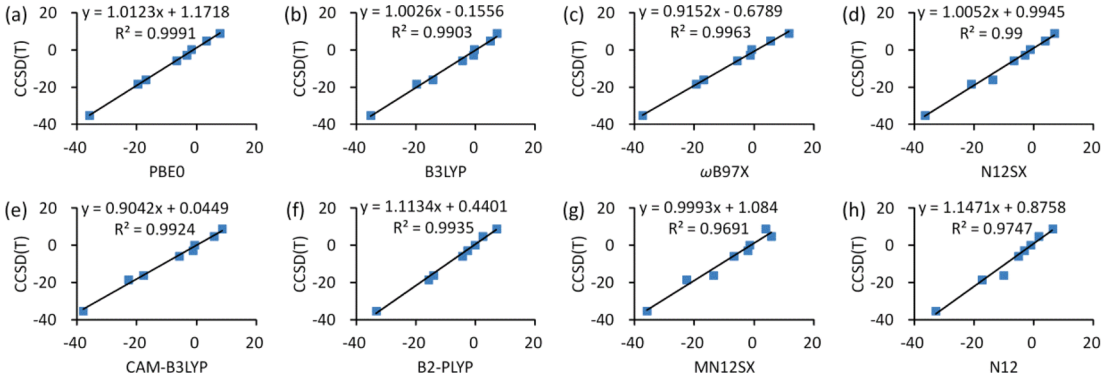

Figure 3. Correlation between reference coupled cluster and DFT (with the eight smallest MUDs after DFT dispersion correction) results for reaction energy.

having the best fitting result is B3LYP with the slope deviating from ideal 1.0 by 0.003 and the intercept deviating from zero by 0.16 kcal/mol. These results of B3LYP and M06-L demonstrate that the quantitative trends of reaction energetics are well followed and that systematic deviations of the energetics are very small. Thus, if considering only the trend performance of various DFs for the energetics of Ru/Rh-mediated reactions, M06-L and B3LYP are certainly the most suitable functionals for reaction barrier and reaction energy calculations, respectively.

3.2.5. Comparison with Previous DFT Calibrations for σ-Bond Activations. Currently in literature, there have been a few explorations of DFT performances concerning σ-bond activations involving several transition metals. Hence, it would be appropriate to compare some related discoveries. Concerning the key H−H bond activation in hydrogenation reactions, the previous DFT calibration work of Neese and his co-workers[77] on Rh(I) involving H−H homolytic cleavage by oxidative addition mechanism and our current results for Rh(III) involving H−H heterolytic cleavage without metal oxidation are complementary in terms of H−H bond activation mode. Comparing the two shared functionals (BP86 and B3LYP) under calibration in these two studies, a common finding is that BP86 consistently underestimates the H−H cleavage barrier compared with B3LYP, while this is not necessarily the case for the reaction energy of H−H cleavage.

Besides H−H activations, another type of σ-bond activation widely explored in DFT calibration studies is C−H activation. In our previous work, we have considered the C−H activation reaction barrier by early transition metal Zr,[96] middle transition metal Re,[95] and late transition metals Rh,[79] Pd,[79] Ir,[79,99] and Pt.[79,99] For early transition metals Zr, M06-2X was found to perform extremely well for C−H activation of σ-bond metathesis mechanism, with an absolute deviation of merely about 0.2 kcal/mol from the reference coupled cluster data.[96] For middle transition metal Re, B2GP-PLYP, TPSS, TPSSh, and LC-ωPBE functionals were found to have the lowest absolute deviations smaller than about 0.7 kcal/mol for both Re(I)-mediated oxidative addition type of C−H activation and Re(III)-mediated σ-bond metathesis type of C−H activation.[95] For late 5d transition metals Ir and Pt, the calibration results indicate that for oxidative addition type of C−H activation B2GP-PLYP, B2-PLYP, PBE0, and TPSSh have the lowest MUDs below about 0.8 kcal/mol.[99] Within various pincer type ligating environments, after considering also late 4d transition metals Rh and Pd in addition to Ir and Pt, the performances of these well performing functionals deteriorate to some extent, and B3LYP was found to keep its good performance and become the best performing functional for all four metals with MUD of about 1.2 kcal/mol.[79] The data in Table 5 of the current study also show that for Rh/Ru-mediated C−H activation reactions (reactions 1a and 1b) B3LYP performs notably well with absolute deviations below 1.2 kcal/mol.

4. CONCLUSIONS

In this work, we assessed the performances of commonly used DFT approximations in calculating activation energies and reaction energies of σ-bond (O−H, C−H, and H−H) activations promoted by two catalytically important 4d platinum group transition metals of Ru and Rh. In all three kinds of σ-bond activations, the selected experimental systems share very similar structures between Ru- and Rh-promoted reactions, which constitutes the basis for an equal footing comparative study between Rh and Ru. For these key elementary reaction processes in organometallic and transition metal catalysis chemistry of Ru and Rh, the DFs under test include 15 commonly used ones and four new ones from the Minnesota series. Generally, the errors of DFT methods for calculating energetics of Ru-/Rh-mediated reactions appear to correlate more with the magnitude of energetics itself than other factors like metal identity.

With the energetics computed by calibrated high level explicitly correlated coupled cluster calculations as reference, there are eight DFs with MUD(Ru), MUD(Rh), and MUD(tot) all less than 2 kcal/mol for activation energy calculations, which are MN12SX < CAM-B3LYP < M06-L < MN12L < M06 < ωB97X < B3LYP < LC-ωPBE (in the order of increasing MUD(tot), similarly hereinafter). For DFT calibrations of reaction energies, the best performing functionals (with all three MUDs < 2 kcal/mol, similarly hereinafter) are PBE0 < CAM-B3LYP ≈ N12SX. DFT empirical dispersion correction was found to be beneficial to most DFs tested in this work, reducing their MUDs to different extents. After including DFT empirical dispersion correction, the best performing DFs for activation energy are ωB97X < B3LYP < CAM-B3LYP < M06-L < M06 < B2-PLYP < LC-ωPBE, while the best performing DFs for reaction energy are PBE0 < B3LYP < ωB97X < B2-PLYP.

On the basis of the above results, PBE0 is clearly the recommendation of functional for reaction energy, both with and without DFT dispersion correction, while for reaction barrier a variable recommendation is more suitable depending on whether the DFT dispersion correction is employed.

DOI: 10.1021/ct5009119
J. Chem. Theory Comput. 2015, 11, 1428−1438

Notably, in the presence of DFT empirical dispersion correction, due to generally good performance, B3LYP and ωB97X can be uniformly recommended for both the reaction energy and reaction barrier calculations. Considering only the trend performance of DFT, while many tested DFs can reliably follow the qualitative trends of calculated energetics in Ru/Rh-promoted σ-bond activations, M06-L and B3LYP with DFT empirical dispersion correction are found to be optimum DFs to most quantitatively follow the trends in reaction barrier and reaction energy calculations, respectively. This additional good characteristics further single B3LYP-D3 out as a reasonable choice for Ru/Rh-promoted σ-bond activation reactions.

■ ASSOCIATED CONTENT

Ⓢ Supporting Information

Five tables of computational results and Cartesian coordinates of all species. This material is available free of charge via the Internet at http://pubs.acs.org.

■ AUTHOR INFORMATION

Corresponding Author

*E-mail: chenh@iccas.ac.cn.

Funding

This work was supported by the National Natural Science Foundation of China (NSFC, Nos. 21290194, 21221002, and 21473215), and Institute of Chemistry, Chinese Academy of Sciences.

Notes

The authors declare no competing financial interest.

■ REFERENCES

(1) Miyaura, N.; Suzuki, A. *Chem. Rev.* **1995**, *95*, 2457−2483.
(2) Zimmer, R.; Dinesh, C. U.; Nandanan, E.; Khan, F. A. *Chem. Rev.* **2000**, *100*, 3067−3126.
(3) Beletskaya, I. P.; Cheprakov, A. V. *Chem. Rev.* **2000**, *100*, 3009−3066.
(4) Negishi, E.; Anastasia, L. *Chem. Rev.* **2003**, *103*, 1979−2017.
(5) Lersch, M.; Tilset, M. *Chem. Rev.* **2005**, *105*, 2471−2526.
(6) Beccalli, E. M.; Broggini, G.; Martinelli, M.; Sottocornola, S. *Chem. Rev.* **2007**, *107*, 5318−5365.
(7) Chen, X.; Engle, K. M.; Wang, D. H.; Yu, J. Q. *Angew. Chem., Int. Ed.* **2009**, *48*, 5094−5115.
(8) Lyons, T. W.; Sanford, M. S. *Chem. Rev.* **2010**, *110*, 1147−1169.
(9) Sehnal, P.; Taylor, R. J.; Fairlamb, I. J. *Chem. Rev.* **2010**, *110*, 824−889.
(10) McDonald, R. I.; Liu, G.; Stahl, S. S. *Chem. Rev.* **2011**, *111*, 2981−3019.
(11) Choi, J.; MacArthur, A. H.; Brookhart, M.; Goldman, A. S. *Chem. Rev.* **2011**, *111*, 1761−1779.
(12) Selander, N.; K, J. S. *Chem. Rev.* **2011**, *111*, 2048−2076.
(13) Suzuki, T. *Chem. Rev.* **2011**, *111*, 1825−1845.
(14) Wu, X. F.; Neumann, H.; Beller, M. *Chem. Rev.* **2013**, *113*, 1−35.
(15) Naota, T.; Takaya, H.; Murahashi, S.-I. *Chem. Rev.* **1998**, *98*, 2599−2660.
(16) Albrecht, M.; van Koten, G. *Angew. Chem., Int. Ed.* **2001**, *40*, 3750−3781.
(17) Trost, B. M.; Toste, F. D.; Pinkerton, A. B. *Chem. Rev.* **2001**, *101*, 2067−2096.
(18) Ritleng, V.; Sirlin, C.; Pfeffer, M. *Chem. Rev.* **2002**, *102*, 1731−1770.
(19) Fagnou, K.; Lautens, M. *Chem. Rev.* **2003**, *103*, 169−196.
(20) Hayashi, T.; Yamasaki, K. *Chem. Rev.* **2003**, *103*, 2829−2844.
(21) van der Boom, M. E.; Milstein, D. *Chem. Rev.* **2003**, *103*, 1759−1792.
(22) de Bruin, B.; Budzelaar, P. H. M.; Gal, A. W. *Angew. Chem., Int. Ed.* **2004**, *43*, 4142−4157.
(23) Pagliaro, M.; Campestrini, S.; Ciriminna, R. *Chem. Soc. Rev.* **2005**, *34*, 837−845.
(24) Trost, B. M.; Frederiksen, M. U.; Rudd, M. T. *Angew. Chem., Int. Ed.* **2005**, *44*, 6630−6666.
(25) Chatterjee, D. *Coordin. Chem. Rev.* **2008**, *252*, 176−198.
(26) Ackermann, L.; Vicente, R. *Top. Curr. Chem.* **2010**, *292*, 211−229.
(27) Samojłowicz, C.; Bieniek, M.; Grela, K. *Chem. Rev.* **2009**, *109*, 3708−3742.
(28) Edwards, H. J.; Hargrave, J. D.; Penrose, S. D.; Frost, C. G. *Chem. Soc. Rev.* **2010**, *39*, 2093−2105.
(29) Lozano-Vila, A. M.; Monsaert, S.; Bajek, A.; Verpoort, F. *Chem. Rev.* **2010**, *110*, 4865−4909.
(30) Colby, D. A.; Bergman, R. G.; Ellman, J. A. *Chem. Rev.* **2010**, *110*, 624−655.
(31) Vougioukalakis, G. C.; Grubbs, R. H. *Chem. Rev.* **2010**, *110*, 1746−1787.
(32) Zhou, M.; Crabtree, R. H. *Chem. Soc. Rev.* **2011**, *40*, 1875−1884.
(33) Ackermann, L. *Chem. Rev.* **2011**, *111*, 1315−1345.
(34) Davies, H. M.; Morton, D. *Chem. Soc. Rev.* **2011**, *40*, 1857−1869.
(35) Dutta, D. K.; Deb, B. *Coord. Chem. Rev.* **2011**, *255*, 1686−1712.
(36) Song, G.; Wang, F.; Li, X. *Chem. Soc. Rev.* **2012**, *41*, 3651−3678.
(37) Arockiam, P. B.; Bruneau, C.; Dixneuf, P. H. *Chem. Rev.* **2012**, *112*, 5879−5918.
(38) Verendel, J. J.; Pamies, O.; Dieguez, M.; Andersson, P. G. *Chem. Rev.* **2014**, *114*, 2130−2169.
(39) Ueura, K.; Satoh, T.; Miura, M. *J. Org. Chem.* **2007**, *72*, 5362−5367.
(40) Ackermann, L.; Pospech, J.; Graczyk, K.; Rauch, K. *Org. Lett.* **2012**, *14*, 930−933.
(41) Palmer, M. J.; Wills, M. *Tetrahedron: Asymmetry* **1999**, *10*, 2045−2061.
(42) Noyori, R. *Angew. Chem., Int. Ed.* **2002**, *41*, 2008−2022.
(43) Clapham, S. E.; Hadzovic, A.; Morris, R. H. *Coord. Chem. Rev.* **2004**, *248*, 2201−2237.
(44) Hedberg, C.; Kallstrom, K.; Arvidsson, P. I.; Brandt, P.; Andersson, P. G. *J. Am. Chem. Soc.* **2005**, *127*, 15083−15090.
(45) Samec, J. S. M.; Backvall, J. E.; Andersson, P. G.; Brandt, P. *Chem. Soc. Rev.* **2006**, *35*, 237−248.
(46) Matharu, D. S.; Morris, D. J.; Clarkson, G. J.; Wills, M. *Chem. Commun.* **2006**, 3232−3234.
(47) Ohkuma, T.; Utsumi, N.; Tsutsumi, K.; Murata, K.; Sandoval, C.; Noyori, R. *J. Am. Chem. Soc.* **2006**, *128*, 8724−8725.
(48) Ikariya, T.; Blacker, A. J. *Acc. Chem. Res.* **2007**, *40*, 1300−1308.
(49) Ito, M.; Ikariya, T. *Chem. Commun.* **2007**, 5134−5142.
(50) Wu, X.; Li, X.; Zanotti-Gerosa, A.; Pettman, A.; Liu, J.; Mills, A. J.; Xiao, J. *Chem.—Eur. J.* **2008**, *14*, 2209−2222.
(51) Wang, C.; Wu, X.; Xiao, J. *Chem. Asian. J.* **2008**, *3*, 1750−1770.
(52) Zhou, H.; Li, Z.; Wang, Z.; Wang, T.; Xu, L.; He, Y.; Fan, Q. H.; Pan, J.; Gu, L.; Chan, A. S. *Angew. Chem., Int. Ed.* **2008**, *47*, 8464−8467.
(53) Chen, F.; Ding, Z. Y.; Qin, J.; Wang, T. L.; He, Y. M.; Fan, Q. H. *Org. Lett.* **2011**, *13*, 4348−4351.
(54) Xie, J. H.; Zhu, S. F.; Zhou, Q. L. *Chem. Rev.* **2011**, *111*, 1713−1760.
(55) Wang, T.; Zhuo, L. G.; Li, Z.; Chen, F.; Ding, Z.; He, Y.; Fan, Q. H.; Xiang, J.; Yu, Z. X.; Chan, A. S. *J. Am. Chem. Soc.* **2011**, *133*, 9878−9891.
(56) Ding, Z. Y.; Chen, F.; Qin, J.; He, Y. M.; Fan, Q. H. *Angew. Chem., Int. Ed.* **2012**, *51*, 5706−5710.
(57) Wang, D. S.; Chen, Q. A.; Lu, S. M.; Zhou, Y. G. *Chem. Rev.* **2012**, *112*, 2557−2590.
(58) Wang, T.; Chen, F.; Qin, J.; He, Y. M.; Fan, Q. H. *Angew. Chem., Int. Ed.* **2013**, *52*, 7172−7176.
(59) Heiden, Z. M.; Rauchfuss, T. B. *J. Am. Chem. Soc.* **2009**, *131*, 3593−3600.

DOI: 10.1021/ct5009119
J. Chem. Theory Comput. 2015, 11, 1428−1438

(60) Chen, Y.; Tang, Y. H.; Liu, S. B.; Lei, M.; Fang, W. H. *Organometallics* **2009**, *28*, 2078−2084.
(61) Lei, M.; Zhang, W.; Chen, Y.; Tang, Y. *Organometallics* **2010**, *29*, 543−548.
(62) Hamid, M. H.; Allen, C. L.; Lamb, G. W.; Maxwell, A. C.; Maytum, H. C.; Watson, A. J.; Williams, J. M. *J. Am. Chem. Soc.* **2009**, *131*, 1766−1774.
(63) Liu, C.; Liao, S.; Li, Q.; Feng, S.; Sun, Q.; Yu, X.; Xu, Q. *J. Org. Chem.* **2011**, *76*, 5759−5773.
(64) Niu, S.; Hall, M. B. *Chem. Rev.* **2000**, *100*, 353−405.
(65) Siegbahn, P. E. M.; Blomberg, M. R. A. *Chem. Rev.* **2000**, *100*, 421−437.
(66) Torrent, M.; Solà, M.; Frenking, G. *Chem. Rev.* **2000**, *100*, 439−493.
(67) Zhou, M.; Andrews, L.; Bauschlicher, C. W., Jr. *Chem. Rev.* **2001**, *101*, 1931−1961.
(68) Baik, M.-H.; Newcomb, M.; Friesner, R. A.; Lippard, S. J. *Chem. Rev.* **2003**, *103*, 2385−2419.
(69) Noodleman, L.; Lovell, T.; Han, W.-G.; Li, J.; Himo, F. *Chem. Rev.* **2004**, *104*, 459−508.
(70) Rotzinger, F. P. *Chem. Rev.* **2005**, *105*, 2003−2037.
(71) Ziegler, T.; Autschbach, J. *Chem. Rev.* **2005**, *105*, 2695−2722.
(72) Cramer, C. J.; Truhlar, D. G. *Phys. Chem. Chem. Phys.* **2009**, *11*, 10757−10816.
(73) Balcells, D.; Clot, E.; Eisenstein, O. *Chem. Rev.* **2010**, *110*, 749−823.
(74) Shaik, S.; Cohen, S.; Wang, Y.; Chen, H.; Kumar, D.; Thiel, W. *Chem. Rev.* **2010**, *110*, 949−1017.
(75) Piacenza, M.; Hyla-Kryspin, I.; Grimme, S. *J. Comput. Chem.* **2007**, *28*, 2275−2285.
(76) Zhao, Y.; Truhlar, D. G. *J. Chem. Theory Comput.* **2009**, *5*, 324−333.
(77) Anoop, A.; Thiel, W.; Neese, F. *J. Chem. Theory Comput.* **2010**, *6*, 3137−3144.
(78) Kang, R. H.; Yao, J. N.; Chen, H. *J. Chem. Theory Comput.* **2013**, *9*, 1872−1879.
(79) Lai, W. Z.; Yao, J. N.; Shaik, S.; Chen, H. *J. Chem. Theory Comput.* **2012**, *8*, 2991−2996.
(80) (a) Perdew, J. P.; Burke, K.; Ernzerhof, M. *Phys. Rev. Lett.* **1996**, *77*, 3865−3868. (b) Ernzerhof, M.; Scuseria, G. E. *J. Chem. Phys.* **1999**, *110*, 5029−5036. (c) Adamo, C.; Barone, V. *J. Chem. Phys.* **1999**, *110*, 6158−6170.
(81) (a) Zhao, Y.; Truhlar, D. G. *J. Chem. Phys.* **2006**, *125*, 194101. (b) Zhao, Y.; Truhlar, D. G. *Theor. Chem. Acc.* **2008**, *120*, 215−241.
(82) Tao, J.; Perdew, J. P.; Staroverov, V. N.; Scuseria, G. E. *Phys. Rev. Lett.* **2003**, *91*, 146401.
(83) (a) Becke, A. D. *J. Chem. Phys.* **1993**, *98*, 5648−5652. (b) Becke, A. D. *Phys. Rev. A* **1988**, *38*, 3098−3100. (c) Lee, C.; Yang, W.; Parr, R. G. *Phys. Rev. B* **1988**, *37*, 785−789.
(84) Karton, A.; Tarnopolsky, A.; Lamere, J.-F.; Schatz, G. C.; Martin, J. M. L. *J. Phys. Chem. A* **2008**, *112*, 12868−12886.
(85) Grimme, S. *J. Chem. Phys.* **2006**, *124*, 034108.
(86) Chai, J.-D.; Head-Gordon, M. *J. Chem. Phys.* **2008**, *128*, 084106.
(87) Handy, N. C.; Cohen, A. J. *Mol. Phys.* **2001**, *99*, 403−412.
(88) Boese, A. D.; Martin, J. M. L. *J. Chem. Phys.* **2004**, *121*, 3405−3416.
(89) Perdew, J. P. *Phys. Rev. B* **1986**, *33*, 8822−8824.
(90) Yanai, T.; Tew, D.; Handy, N. *Chem. Phys. Lett.* **2004**, *393*, 51−57.
(91) (a) Vydrov, O. A.; Heyd, J.; Krukau, A. V.; Scuseria, G. E. *J. Chem. Phys.* **2006**, *125*, 074106. (b) Vydrov, O. A.; Scuseria, G. E. *J. Chem. Phys.* **2006**, *125*, 234109.
(92) Peverati, R.; Truhlar, D. G. *J. Chem. Theory Comput.* **2012**, *8*, 2310−2319.
(93) Peverati, R.; Truhlar, D. G. *Phys. Chem. Chem. Phys.* **2012**, *14*, 13171−13174.
(94) Peverati, R.; Truhlar, D. G. *Phys. Chem. Chem. Phys.* **2012**, *14*, 16187−16191.
(95) Sun, Y. H.; Chen, H. *J. Chem. Theory Comput.* **2014**, *10*, 579−588.
(96) Sun, Y. Y.; Chen, H. *J. Chem. Theory Comput.* **2013**, *9*, 4735−4743.
(97) Chen, H.; Lai, W. Z.; Shaik, S. *J. Phys. Chem. Lett.* **2010**, *1*, 1533−1540.
(98) Kang, R. H.; Chen, H.; Shaik, S.; Yao, J. N. *J. Chem. Theory Comput.* **2011**, *7*, 4002−4011.
(99) Kang, R. H.; Lai, W. Z.; Yao, J. N.; Shaik, S.; Chen, H. *J. Chem. Theory Comput.* **2012**, *8*, 3119−3127.
(100) Frisch, M. J.; Trucks, G. W.; Schlegel, H. B.; Scuseria, G. E.; Robb, M. A.; Cheeseman, J. R.; Scalmani, G.; Barone, V.; Mennucci, B.; Petersson, G. A.; Nakatsuji, H.; Caricato, M.; Li, X.; Hratchian, H. P.; Izmaylov, A. F.; Bloino, J.; Zheng, G.; Sonnenberg, J. L.; Hada, M.; Ehara, M.; Toyota, K.; Fukuda, R.; Hasegawa, J.; Ishida, M.; Nakajima, T.; Honda, Y.; Kitao, O.; Nakai, H.; Vreven, T.; Montgomery, J. A., Jr.; Peralta, J. E.; Ogliaro, F.; Bearpark, M.; Heyd, J. J.; Brothers, E.; Kudin, K. N.; Staroverov, V. N.; Kobayashi, R.; Normand, J.; Raghavachari, K.; Rendell, A.; Burant, J. C.; Iyengar, S. S.; Tomasi, J.; Cossi, M.; Rega, N.; Millam, J. M.; Klene, M.; Knox, J. E.; Cross, J. B.; Bakken, V.; Adamo, C.; Jaramillo, J.; Gomperts, R.; Stratmann, R. E.; Yazyev, O.; Austin, A. J.; Cammi, R.; Pomelli, C.; Ochterski, J. W.; Martin, R. L.; Morokuma, K.; Zakrzewski, V. G.; Voth, G. A.; Salvador, P.; Dannenberg, J. J.; Dapprich, S.; Daniels, A. D.; Farkas, O.; Foresman, J. B.; Ortiz, J. V.; Cioslowski, J.; Fox, D. J. *Gaussian 09*, revision C.01; Gaussian, Inc.: Wallingford, CT, 2009.
(101) Dunning, T. H., Jr. *J. Chem. Phys.* **1989**, *90*, 1007−1023.
(102) Dunning, T. H., Jr.; Peterson, K. A.; Wilson, A. K. *J. Chem. Phys.* **2001**, *114*, 9244−9253.
(103) Peterson, K. A.; Figgen, D.; Dolg, M.; Stoll, H. *J. Chem. Phys.* **2007**, *126*, 124101.
(104) Grimme, S.; Antony, J.; Ehrlich, S.; Krieg, H. *J. Chem. Phys.* **2010**, *132*, 154104.
(105) Goerigk, L.; Grimme, S. *J. Chem. Theory Comput.* **2011**, *7*, 291−309.
(106) Chai, J.-D.; Head-Gordon, M. *Phys. Chem. Chem. Phys.* **2008**, *10*, 6615−6620.
(107) Werner, H. J.; Knowles, P. J.; Knizia, G.; Manby, F. R.; Schütz, M.; Celani, P.; Korona, T.; Lindh, R.; Mitrushenkov, A.; Rauhut, G.; Shamasundar, K. R.; Adler, T. B.; Amos, R. D.; Bernhardsson, A.; Berning, A.; Cooper, D. L.; Deegan, M. J. O.; Dobbyn, A. J.; Eckert, F.; Goll, E.; Hampel, C.; Hesselmann, A.; Hetzer, G.; Hrenar, T.; Jansen, G.; Köppl, C.; Liu, Y.; Lloyd, A. W.; Mata, R. A.; May, A. J.; McNicholas, S. J.; Meyer, W.; Mura, M. E.; Nicklass, A.; O'Neill, D. P.; Palmieri, P.; Pflüger, K.; Pitzer, R.; Reiher, M.; Shiozaki, T.; Stoll, H.; Stone, A. J.; Tarroni, R.; Thorsteinsson, T.; Wang, M.; Wolf, A. *MOLPRO*, version 2010, a package of ab initio programs; see http://www.molpro.net.
(108) Adler, T. B.; Knizia, G.; Werner, H.-J. *J. Chem. Phys.* **2007**, *127*, 221106.
(109) Knizia, G.; Adler, T. B.; Werner, H.-J. *J. Chem. Phys.* **2009**, *130*, 054104.
(110) (a) Weigend, F. *J. Comput. Chem.* **2008**, *29*, 167−175. (b) The def2-AQZVPP/JKFIT basis set contains one even-tempered diffuse function for each primitive set of Weigend's def2-QZVPP/JKFIT in ref 110a and was taken from the MOLPRO basis set library.
(111) (a) Weigend, F. *Phys. Chem. Chem. Phys.* **2002**, *4*, 4285−4291. (b) The aug-cc-pVTZ/JKFIT basis set contains one even-tempered diffuse function for each primitive set of Weigend's cc-pVTZ/JKFIT in ref 111a and was taken from the MOLPRO basis set library.
(112) Hill, J. G.; Platts, J. A. *J. Chem. Phys.* **2008**, *129*, 134101.
(113) Weigend, F.; Köhn, A.; Hättig, C. *J. Chem. Phys.* **2002**, *116*, 3175−3183.
(114) Valeev, E. F. *Chem. Phys. Lett.* **2004**, *395*, 190−195.
(115) Hill, J. G.; Peterson, K. A. *J. Chem. Theory Comput.* **2012**, *8*, 518−526.
(116) Schwenke, D. W. *J. Chem. Phys.* **2005**, *122*, 014107.
(117) Hill, J. G.; Peterson, K. A.; Knizia, G.; Werner, H.-J. *J. Chem. Phys.* **2009**, *131*, 194105.

DOI: 10.1021/ct5009119
J. Chem. Theory Comput. 2015, 11, 1428−1438

(118) Knizia, G.; Werner, H.-J. *J. Chem. Phys.* **2008**, *128*, 154103.
(119) Hill, J. G. *J. Comput. Chem.* **2013**, *34*, 2168−2177.

DOI: 10.1021/ct5009119
J. Chem. Theory Comput. 2015, 11, 1428−1438